



Contents lists available at ScienceDirect

## Journal of King Saud University – Science

journal homepage: [www.sciencedirect.com](http://www.sciencedirect.com)

Original article

## Conformal geometry of the turtle shell

Rabha W. Ibrahim <sup>a,b,\*</sup><sup>a</sup> Informetrics Research Group, Ton Duc Thang University, Ho Chi Minh City, Viet Nam<sup>b</sup> Faculty of Mathematics & Statistics, Ton Duc Thang University, Ho Chi Minh City, Viet Nam

## ARTICLE INFO

## Article history:

Received 15 July 2019

Revised 12 February 2020

Accepted 20 February 2020

Available online 4 March 2020

## Keywords:

Conformal geometry  
fractional differential operator  
shell morphology  
fractional calculus  
analytic function  
unit disk  
fractional entropy

## ABSTRACT

Characteristic between species is an important feature of animal investigation and preservation. For turtles, different analysis is possibly respected implements for identification. Shell shape is an essential component of analysis and classification in turtles and can be simply styled and measured by conformal geometric (CG). Here, we focus on the shell shape of a Southeast Asian leaf turtle by utilizing CG approaches. CG approaches recognized important differences in shell shape of turtles by using the convexity part of the shell structure. The symmetry of the sail shape in this type of turtles is a very important recognition. Therefore, we introduce a symmetric differential operator using its roots to study the shell shape. 2D printing tool paths are recognized for these shells.

© 2020 The Author(s). Published by Elsevier B.V. on behalf of King Saud University. This is an open access article under the CC BY-NC-ND license (<http://creativecommons.org/licenses/by-nc-nd/4.0/>).

## 1. Introduction

The turtle shell is made up of various bony components, usually called after related bones in new vertebrates, and a sequence of keratin sautes (a thickened bony plate on a turtle's shell) which are furthermore exclusively entitled. Some of those bones that create the upper of the shell are changed from surface to another. Our study is based on the convex part of the shell structure of a turtle, which is called the carapace involving of the animal's hardened ribs welded with the dermal bone. The progress (growth) of the turtle's shell is unique because of how the carapace characterizes changed backs and ribs (Romer, 1956; Zangerl, 1969; Lyson et al., 2013; Cordero, 2017).

The geometry of the shell can be explained in two dimensions, the mechanism is essentially three dimensional: the center of gravity  $G$  is formulated not only by the central cross-section but by the whole body. Therefore, the structure must be involved in solid cylinder planar discs to imply convex, homogenous three-dimensional objects with just one stable and equilibrium may occur (Abelson and Andrea, 1986).

In this work, our contribution is to deliver a new geometric representation of the shell shape of a Southeast Asian turtle by

utilizing CG method. This method accepted important differences in shell shape of turtles, like the symmetry, stability and equilibrium of shells. The method is based on formulating a symmetric differential operator using its roots to study the shell shape. 2D printing tool paths are recognized for these shells. We shall use Wolfram Mathematica 11.2 and the Javascript conformal map viewer to code our algorithm.

## 2. Related works

Domokos and Varkonyi (2007) introduced a geometric structure of the turtle shell in three steps: (i) transverse, this step is in a polar coordinate system; (ii) longitudinal, this step is describing side- and top-view contours of the shell; (iii) 3D- representing, this step is a surface model combining a series of horizontal and vertically scaled versions of the main transverse section, coinciding the longitudinal contours. They established the model parameters to separate measured turtle shapes, and then to control the equilibrium class of the 3D-model

$$P(\alpha, r, \kappa) = \frac{p_0}{\cos(\alpha)}, \quad \alpha \in \left[-\frac{\pi}{2}, \frac{\pi}{2}\right],$$

where  $P$  is the polar system,  $p_0$  is a scaling factor and  $\kappa$  is the contour of the cross-section with radius  $r$ . More generalization of the above construction is given by Krauss et al. (2009). They added other factors such as length, viscosity and a geometric factor  $\varepsilon$  to recognize the zigzag structure.

\* Address: Informetrics Research Group, Ton Duc Thang University, Ho Chi Minh City, Viet Nam; Faculty of Mathematics & Statistics, Ton Duc Thang University, Ho Chi Minh City, Viet Nam.

E-mail address: [rabhaibrahim@tdtu.edu.vn](mailto:rabhaibrahim@tdtu.edu.vn)

Zhang et al. (2012) studied the dynamical representation of the shell by using optimization and numerical methods (2-D finite element model). P2 is a two-dimensional problem (Dirichlet problem)

$$P(2 - D) : \begin{cases} \mu_{xx}(x,y) + \mu_{yy}(x,y) = \varphi(x,y) & \text{in } \Omega, \\ \mu = 0 & \text{on } \partial\Omega, \end{cases}$$

where  $\Omega$  is a connected open region in the  $(x,y)$  plane whose boundary  $\partial\Omega$  is a smooth domain (in our model, we shall suggest the open unit disk), and  $\mu_{xx}$  and  $\mu_{yy}$  represent to the second derivatives with respect to  $x$  and  $y$ , respectively. Fig. 1 shows the structures of the turtle shell for Domokos and Varkonyi (2007) and Zhang et al. (2012) respectively.

Djumas et al. (2016) established a new method by utilizing a geometric topological method (topological interlocking). The idea is based on the segmentation of solid materials into particularly aimed, discrete matching units which interlock in 3-D to form an assembly. In this method, each component is controlled by the geometry of its neighbouring components, given that the assembly a tool to have load-bearing mechanical integrity without the need for connectors or folders. A global control in the form of a frame, angle ties or tension supports is required to keep the general structure.

Recently, by using statistical methods in data science (such as segmentation, hypothesis, etc.), Hosseini et al. (2019) and Van Le et al. (2019) provided a 3-D geometrical structure of the shell. Ferreira and Werneburg (2019), based on 3D reforms method in geometry, they proposed a theoretical model for a turtle with a complete shell. The significant stage toward the accepting the growth of those muscles in turtles. Finally, Brejcha et al. (2019) studied the color of the skin based on the Fourier analysis of some spatial distributions. The Fourier analysis of such a function ( $\varphi$ ) is given by the formula

$$\varphi(x) = \sum_{n=-\infty}^{\infty} K_n e^{2\pi i(\frac{\eta}{\lambda})x} = \sum_{n=-\infty}^{\infty} \hat{\varphi}(\eta_n) e^{2\pi i\eta_n x} \Delta\eta.$$

We note that there are three original shapes for the turtle shell, Diamond shell, Leaf shell and Flap shell (see Fig. 2), where other types are hybrids of these three types. Our study focuses on the leaf turtle shell.

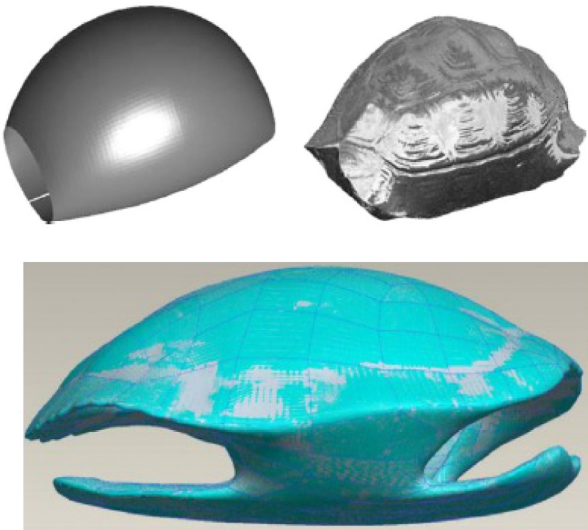


Fig. 1. Geometric methods which are given in Domokos and Varkonyi (2007) and Zhang et al. (2012) respectively.



Fig. 2. Shapes of turtle shell.

### 3. Methodology

In this section, we illustrate some important concepts that will be used in the sequel.

#### 3.1. DDO

We deliver the new DDO in the open unit disk. Let  $\Lambda$  be the class of analytic function formulated by

$$\varphi(z) = z + \sum_{n=2}^{\infty} \varphi_n z^n, \quad z \in U = \{z : |z| < 1\}. \tag{1}$$

This class of analytic functions provides the geometric construction of any conformal mappings (Duren, 1983). This class involves the special class of analytic functions called the univalent functions, which implies stalikeness, convexity and concavity of conformal mappings in the open unit disk.

For a function  $\varphi \in \Lambda$ , we present a new differential operator in  $U$

$$\begin{aligned} \Delta_\beta^0 \varphi(z) &= \varphi(z) \\ \Delta_\beta^1 \varphi(z) &= \left(\frac{\beta}{\beta}\right) z \varphi'(z) - \left(1 - \frac{\beta}{\beta}\right) z \varphi'(-z), \end{aligned} \tag{2}$$

where for  $m$  iteration, the operator (2) becomes:

$$\begin{aligned} \Delta_\beta^m \varphi(z) &= \Delta_\beta \left( \Delta_\beta^{m-1} \varphi(z) \right) \\ &= z + \sum_{n=2}^{\infty} \left( n \left( \frac{\beta}{\beta} - \left(1 - \frac{\beta}{\beta}\right) (-1)^n \right) \right)^m \varphi_n z^n, \end{aligned}$$

where  $\beta$  is a complex number. Table 1 shows some examples which are useful in our study.

Domokos and Varkonyi (2007) have classified turtle shells into three classes depending on the equilibrium points in the two planes of reflection symmetry such that the  $y$ -coordinate is to be calculated (Fig. 3).

#### 3.2. Energy

In this work, the algorithm is based on conformal mappings in the open unit disk. Therefore, the energy should take its value as a complex number. Follow the technique of complex fractional entropy (Ibrahim and Darus, 2018), we have construct the value of energy. Moreover, since the study is in the open unit disk, therefore, at best value of the energy does not exceed one.

Let  $\mathbf{Z}$  be the set of  $N$ - roots of DDO (2) in  $U$ ,

$$\mathbf{Z} = \{\eta_1, \dots, \eta_N\} \subset U.$$

Hence, the total information is a complex vector determining from the complex fractional entropy

$$I_\rho(\eta) = \sum_{k=1}^N \frac{\eta_k}{\rho - 1}, \quad \rho \neq 1, \eta \in \mathbf{Z}, \tag{3}$$

**Table 1**  
Examples of  $\Delta_v^m(z), z \in \mathbb{U}$ . The roots are illustrated in symmetric structures.

$\varphi(z)$	$\Delta_v^m(z), v = \frac{\beta}{\alpha}$	Roots in the complex plane
$\frac{z}{1-z}$	$\Delta_{0.2}^1 = \frac{0.2z}{(1-z)^2} + \frac{0.8z}{(1+z)^2}$	$0, 0.6 \pm 0.8i$
-	$\Delta_{0.8}^1 = \frac{0.8z}{(1-z)^2} + \frac{0.2z}{(1+z)^2}$	$0, -0.6 \pm 0.8i$
$\frac{z}{(1-z)^2}$	$\Delta_{0.2}^1 = -\frac{0.2z(1+z)}{(z-1)^3} + \frac{0.8z(1-z)}{(1+z)^3}$	$0, 0.2 \pm 0.4i, 1 \pm 2i$
-	$\Delta_{0.8}^1 = -\frac{0.8z(1+z)}{(z-1)^3} + \frac{0.2z(1-z)}{(1+z)^3}$	$0, -0.2 \pm 0.4i, -1 \pm 2i$

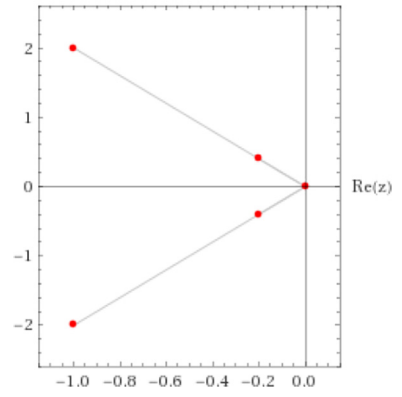
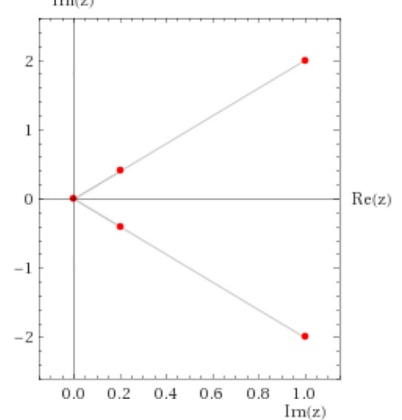
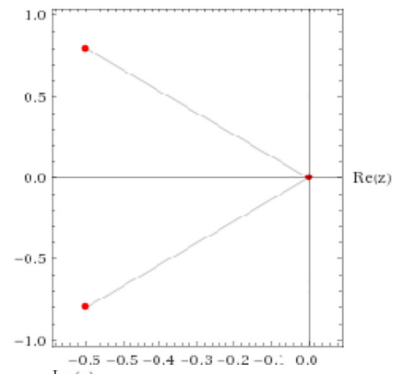
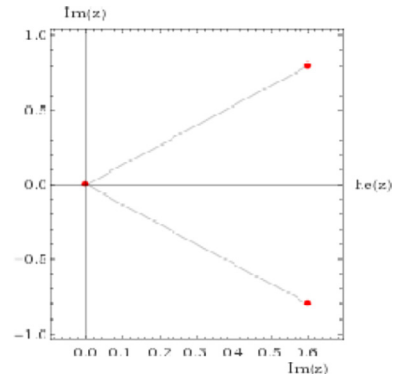
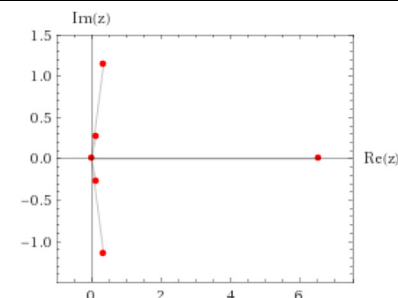
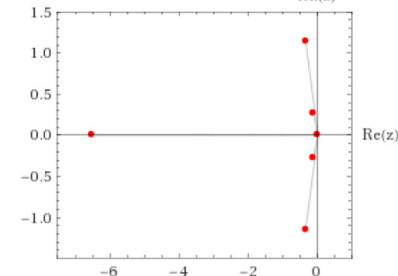


Table 1 (continued)

$\varphi(z)$	$\Delta_v^m(z), v = \frac{\beta}{\beta}$	Roots in the complex plane
$\frac{z}{(1-z)^2}$	$\Delta_{0.2}^1 = \frac{0.2z(1+2z)}{(1-z)^4} - \frac{0.8z(2z-1)}{(1+z)^4}$	$0, 0.1 \pm 0.2i, 0.3 \pm 1i$
-	$\Delta_{0.8}^1 = \frac{0.8z(1+2z)}{(1-z)^4} - \frac{0.2z(2z-1)}{(1+z)^4}$	$0, -0.1 \pm 0.2i, -0.3 \pm 1i$

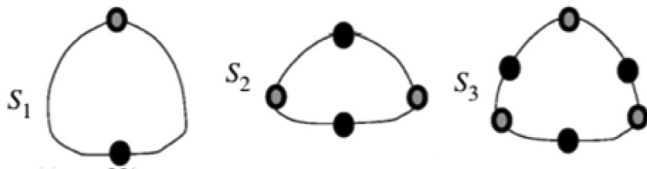


Fig. 3. Classes of turtle shall in (Domokos and Varkonyi, 2007). Class  $S_1$  is signified by a rather small domain, tall turtles are unusually close to  $S_1$ , i.e. they tend to be monochromatic and  $S_2$  for mote symmetrical shells including the flap shape, the popularity of standard turtle’s shell drops into  $S_3$ .

Moreover, large amount of information occurs from both theoretical investigations and numerical calculations from (3). The stability of (3) is realized by the energy equation

$$\Xi_\rho = \frac{I_\rho(\eta)\bar{I}_\rho(\eta)}{N}, \tag{4}$$

where  $\bar{I}_\rho(\eta)$  is the conjugate of  $I_\rho(\eta)$ . The energy gives a tool for studying the dynamics of DDO. Table 2 shows the distribution of our results for some useful conformal mappings. These conformal mappings are utilized to describe the shell shape under the operator (2). The first function  $\varphi(z) = z + 0.9z^3$  represents to  $S_1$  model, the second mapping ( $\varphi(z) = z/(1-z)$ ) acts as the  $S_2$ -type and the third mapping ( $\varphi(z) = z/(1-z)^2$ ) performs the  $S_3$ -design (see Fig. 4). Experimentally, the value  $\rho = 3$  implies a higher energy for the system ( $\Xi_\rho \approx 1$  for  $S_2$ ). This method implies guarantee the energy is less or equal to 1, because of the value of  $\rho$ .

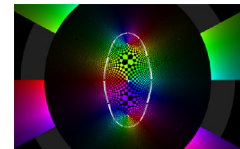

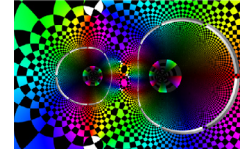
### 3.3. Algorithm

The algorithm can be recognized by the following steps.

- Input the Kobe function (signal presentation of the shell)  $\varphi(z) = z/(1-z)^n, n = 1, 2, 3, \dots, N, \beta, m = 1, \dots, K$ ;
- Operate the signal of the shell by using the symmetric operator DDO which is given in Eq.(2);

Table 2

The energy of DDO (2) for  $\rho = 3$ . In our discussion,  $S_1$  distributes the energy equally,  $S_2$  the energy is high on the boundary of the unit disk, and  $S_3$  shows the distribution for different roots are not equal on the shell shape.

$\varphi(z)$	$\Xi_\rho(\eta), \rho = 3$	2-D energy distribution
$S_1 : z + 0.9z^3$	$\Xi_3 = \frac{0.608^2}{2} = 0.184$ (two roots)	
$S_2 : \frac{z}{1-z}$	$\Xi_3 \approx 1$ (two roots)	
$S_3 : \frac{z}{(1-z)^2}$	$\Xi_3 = \frac{1.44}{4} = 0.36$ (4 roots)	

- Find all the roots of DDO inside the unit disk (we ignore the roots outside the unit disk);
- Congruent these roots with the point of the shell to recognize the type  $S_1, S_2$  and  $S_3$ ;
- Evaluate the energy in Eq.(4)

### 4. Discussion

Fig. 4 shows the comparison with the suggested geometry in (Domokos and Varkonyi, 2007) and the symmetric distribution of roots in the open unit disk for the operating (2). Obviously, we can see the congruence of roots in left and right distributions for  $S_2$  and  $S_3$ . For  $S_1$ , we suggested the function  $\varphi(z) = z + 0.9z^3$ , where

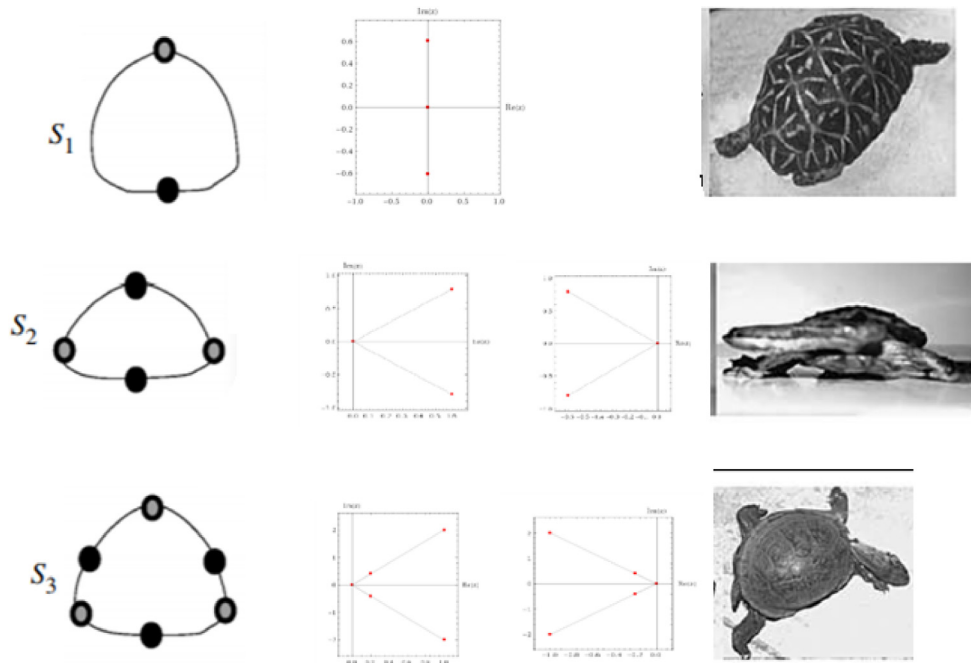


Fig. 4. Comparison between Domokos and Varkonyi (2007) geometry and our algorithm.

this function gives two imaginary roots  $r_{1,2} = \pm 0.608i$  in the open unit disk differ from the origin (zero root). By experimental rotation, to get symmetric shape, we have considered  $v = \frac{\beta}{\bar{\beta}} = 0.2$  and  $m = 1$  for all  $S_j$ ,  $j = 1, 2, 3$ .

The advantageous of this algorithm are recognized as follows:

- The conformal segments involve a set of center, radii and roots;
- DDO (2) is normalized in the open unit disk; therefore, no need to use a weighted space;
- The energy is determined by the roots of DDO in the open unit disk; therefore, there is no wasting of energy (high accuracy of evaluation);
- This technique is iterative, hence the DDO collects the connected data regarding the shape of a shell.

## 5. Conclusion

Shell shape is an essential component of analysis and classification in turtles. We introduced a new study based on the conformal mappings theory by formulating a new symmetric differential operator in the open unit disk. We considered the roots of operator (2), that is:  $\Delta_v^m \varphi_i(z) = 0$ ,  $i = 1, 2, 3$ , where  $v = \beta/\bar{\beta}$  and  $\varphi_1(z) = z + 0.9z^3$  represents to  $S_1$  model, the second mapping  $\varphi_2(z) = z/(1-z)$  symbolizes the  $S_2$ -type and the third mapping  $\varphi_3(z) = z/(1-z)^2$  introduces the  $S_3$ -type. We conclude that the roots of the  $\Delta_v^m \varphi_i(z)$  coincided with the shapes that recognized in (Domokos and Varkonyi, 2007). Moreover, we examined the stability and the energy by using entropy with complex values.

## Declaration of Competing Interest

The authors declare that they have no known competing financial interests or personal relationships that could have appeared to influence the work reported in this paper.

## Acknowledgments

The author wishes to express his profound gratitude to the anonymous referee for his/her careful reading of the manuscript and the very useful comments that have been implemented in the final version of the manuscript.

## References

- Abelson, H., Andrea, A.D., 1986. *Turtle Geometry: The Computer as a Medium for Exploring Mathematics*. MIT Press.
- Brejcha, J. et al., 2019. Body coloration and mechanisms of colour production in Archelosauria: the case of deirocheline turtles. *Royal Society open science* 6(7), 190319, 556–670.
- Cordero, G.A., 2017. The Turtle's Shell. *Curr. Biol.* 27 (5), R168–R169.
- Djumas, Lee et al., 2016. Enhanced mechanical performance of bio-inspired hybrid structures utilising topological interlocking geometry. *Sci. Rep.* 6, 26706.
- Domokos, G., Varkonyi, P.L., 2007. Geometry and self-righting of turtles. *Proc. R. Soc. B: Biol. Sci.* 275 (1630), 11–17.
- Duren P., 1983. *Univalent Functions, Grundlehren der mathematischen Wissenschaften*; 259 Springer-Verlag, New York Inc..
- Ferreira, G.S., Werneburg, I., 2019. Evolution, diversity, and development of the craniocervical system in turtles with special reference to jaw musculature. In: Ziermann, J., Diaz, R., Jr, Diogo, R. (Eds.), *Heads, Jaws, and Muscles. Fascinating Life Sciences*. Springer, Cham.
- Hosseini, Maryam S. et al., 2019. Analysis of bioinspired non-interlocking geometrically patterned interfaces under predominant mode I loading. *J. Mech. Behav. Biomed. Mater.* 96, 244–260.
- Ibrahim, R.W., Darus, Maslina, 2018. Analytic study of complex fractional Tsallis' entropy with applications in CNNs. *Entropy* 20 (10), 722.
- Krauss, Stefanie et al., 2009. Mechanical function of a complex three-dimensional suture joining the bony elements in the shell of the red-eared slider turtle. *Adv. Mater.* 21 (4), 407–412.
- Lyson, Tyler R et al., 2013. Homology of the enigmatic nuchal bone reveals novel reorganization of the shoulder girdle in the evolution of the turtle shell. *Evolution Develop.* 15 (5), 317–325.
- Romer, A.S., 1956. *Osteology of the Reptiles*. Univ of Chicago Press.
- Van Le, Tu, et al., 2019. A comprehensive review of selected biological armor systems—from structure-function to bio-mimetic techniques. *Compos. Struct.* 111–172.
- Zangerl, R., 1969. The turtle shell. In: Gans, C., Bellairs, D.d'A., Parsons, T.A. (Eds.), *Biology of the Reptilia*, 1, Morphology A. Academic Press, London, pp. 311–340.
- Zhang, Wei et al., 2012. Numerical study of the mechanical response of turtle shell. *J. Bionic Eng.* 9 (3), 330–335.